www.dergipark.gov.tr
ISSN:2148-3736
El-Cezerî Fen ve Mühendislik Dergisi
Cilt: 5, No: 1, 2018 (243-250)

El-Cezerî Journal of Science and Engineering
Vol: 5, No: 1, 2018 (243-250)

ECJSE

**Research Paper / Makale**

# Solid Particle Erosion Effects on Surface Plastic Deformation of Alüminum Alloy

**Hakan SEZER[1] , Sinan FIDAN[2]**

[1]Kocaeli University, Institute of Science, Aviation Knowledge and Technology, 41380,Kocaeli, TURKEY
[2] Kocaeli University, Faculty of Aeronautics and Astronautics, Department of Airframe & Powerplant, 41285, Kartepe-Kocaeli, Turkey
hakann_sezerr@hotmail.com sinanfidandr@yahoo.com

**Abstract:** Aluminum alloys are one of the most common materials used in aircraft structural part production. Moreover, high cruising speeds of aircrafts resulted with high velocity impacts of micro hard particles such as dust, fly ash, impact ice and rain droplets. These hard particles involved in atmospheric air concentration cause repeated impacts on surface Extruded AA6082-T6 aluminum alloy sheets were subjected to solid particle erosion tests. Solid particle erosion tests were performed according to ASTM G 76 standard. Abrasive particles with various particle sizes blasted to surfaces of AA6082-T6 aluminum alloy test coupons. Solid particle erosion tests accomplished at normal incidence (impact angle:90°) with blast pressure of 3 Bar. Average roughness (Ra), average distance between the highest peak and lowest valley in each sampling length (Rz) and 3D surface topography maps and erosive wear rates of AA6082-T6 aluminum alloy test coupons were obtained before and after solid particle erosion tests. Correlations between erosion crater volume and mass loss were discussed.

**Keywords:** Plastic deformation, Solid particle erosion, Aluminum alloy, Erosion rate, Surface topography.

# Alüminyum Alaşımının Yüzey Plastik Deformasyonunda Katı Parçacık Erozyon Etkisi

**Özet:** Alüminyum alaşımları, uçak yapısal parça üretiminde kullanılan en yaygın malzemelerden biridir. Üstelik uçakların yüksek seyir hızları, toz, uçucu kül, darbe buzu ve yağmur damlacıkları gibi mikro sert parçacıkların yüksek hız etkileriyle sonuçlanır. Atmosferik hava konsantrasyonunda yer alan bu sert parçacıklar, yüzey üzerinde tekrarlanan darbelere neden olur. Ekstrüde AA6082-T6 alüminyum alaşım tabakaları katı parçacık erozyon testlerine tabi tutuldu. Katı parçacık erozyon testleri ASTM G 76 standardına göre gerçekleştirildi. Çeşitli parçacık boyutlarına sahip aşındırıcı partiküller, AA6082-T6 alüminyum alaşım test kuponlarının yüzeylerine püskürtüldü. Katı parçacık erozyon testleri, 3 Barlık patlama basıncı ile normal insidansa (darbe açısı: 90 °) ulaşıldı. AA6082-T6 alüminyum alaşımlı test kuponlarının ortalama yüzey pürüzlülüğü (Ra), her örnekleme uzunluğundaki (Rz) en yüksek tepe ve en düşük vadiye arasındaki ortalama mesafe ve 3D yüzey topoğrafya haritaları ve eroziv aşınma oranları katı partikül erozyon testlerinden önce ve sonra elde edildi. Erozyon krater hacmi ile kütle kaybı arasındaki korelasyonlar tartışıldı.

**Anahtar kelimeler:** Plastik Deformasyon, Katı Partikül Erozyonu, Alüminyum Alaşımı, Erozyon Hızı, Yüzey topoğrafyası.

*How to cite this article*
Sezer, H., Fidan, S., "Solid Particle Erosion Effects On Surface Plastic Deformation Of Alüminum Alloy " El-Cezerî Journal of Science and Engineering, 2018, 5(1); 243-250.

*Bu makaleye atıf yapmak için*
Sezer, H, Fidan, S., *"Alüminyum Alaşımının Yüzey Plastik Deformasyonunda Katı Parçacık Erozyon Etkisi "* El-Cezerî Fen ve Mühendislik Dergisi 2018, 5(1); 243-250.

## 1. Introduction

Impingement of abrasive particles with high velocity air or liquid against the surface of a target material causes deformation and material removal. This phenomenon called erosive wear. Shape, size, morphology, hardness and density of the particles, physical and chemical properties of the target materials and the operational parameters affect the complexity of the deformation and damage behavior of materials under repeated impacts of abrasive particles. Erosion of materials due to the impingement of solid particles is one form of wear degradation that jeopardizes integrity of the flow boundaries and functionality of moving components in particle-contained flows [1].

Solid particle erosion involves the impact of small high speed particles on a target, causing surface damage and material removal that, on a per particle basis, occurs on a very small scale and for a very short time. This, together with the irregularity of particle shape and size typically found in erodent powders, and the complexity of the deformation and damage behavior of materials under impact loadings, makes it very challenging to identify the micro- mechanisms of erosion that lead to macro-scale material loss. These complexities have led researchers to take simplified approaches in order to understand erosion mechanisms in ductile materials[2].

Aluminum and its alloys are widely used in a wide variety of applications. Aluminum's main advantages include: lightness, high specific strength, high thermal and electrical conductivities, good formability, excellent machinability, diversity of aluminum alloys, extensive range of forms and processing options (e.g. rolling, extrusions, stampings, forgings and castings) and suitability for a diverse range of joining techniques, surface treatments and recyclability [3]. Aluminum alloys are materials of choice in many engineering applications because of their excellent combination of high specific strength, ductility, thermal conductivity and corrosion resistance. Nevertheless, due to their relative softness and low wear resistance, aluminum alloys are not generally employed in tribological applications [4].

Solid particle erosion is a progressive phenomenon that can result with surface degradation and material removal. It occurs in a wide variety of materials and assemblies such as aircraft airframes, radomes, leading edge control surfaces etc. Aluminum alloys are one of the most common materials used in aircraft structural part production. Moreover, high cruising speeds of aircrafts resulted with high velocity impacts of micro hard particles such as dust, fly ash, impact ice and rain droplets. These hard particles involved in atmospheric air concentration cause repeated impacts on surface. Hence, it is crucial to investigate the surface induced damages due to repeated impacts of solid particles.

## 2. Materials and Methods

Extruded AA6082-T6 aluminum alloy sheets with a nominal thickness of 3 mm were kindly supplied from ASAŞ-TURKEY. The samples were cut into square coupon test samples, with a dimension of 50 mm×50 mm. Table 1 provides the mechanical properties of AA6082-T6 aluminum alloy, according to the manufacturer's declaration.

Table 1. AA6082-T6 aluminum alloy sheet properties

| | |
|---|---|
| $R_m$ Tensile ($N/mm^2$ min.) | 290 |
| $R_{p0,2}$ Yielding ($N/mm^2$ min.) | 250 |
| HBW typical value | 95 |
| Heat treatment temperature (ºC) | 175-185 |
| Heat treatment duration (hours) | 8-6 |
| Hardness (Brinell HB) | 85-90 |
| A50 Elongation min. | 6 |

Solid particle erosion tests were performed in accordance with the ASTM G76 standard. The alumina particles are used as an erodent during the particle erosion experiments were, with 3 distinct particle size of 60 mesh (212-300 µm); 80 mesh (150-212 µm) and 120 mesh (90-250µm) respectively..

The particle erosion tests were performed at normal impingement angle (90°). Erosive particles are blasted under air pressure of 3 bar through a ceramic nozzle with an inner diameter of 7 mm in a specially designed air jet test rig. The AA6082-T6 aluminum samples were located at a distance of 20 mm from the nozzle exit (stand-off distance). 40 gr. of erodent for each alumina particle size was blasted under same test conditions. Three reputations were carried out for each test parameter. The mean value of three experiments was taken into account for every test condition. The average mass loss was presented. Before the particle erosion tests, sample surfaces were cleaned with air blasting and acetone in order to achieve clean surface. Mass loss was measured by using an electronic balance with an accuracy of ± 0,1 mg.

The erosion test rig used in this study is illustrated in Fig 1. Accelerated particles were impacted the sample surface, which can be located at desired distance from nozzle and placed at various impingement angles (15°-90°) by adjustable sample holder shown in Fig 1. Particle impact velocity was measured by using the double disc method. Under 3 bar air blast pressure; particles with a size of 60 mesh has an impact velocity of 64 m/s; 80 mesh has an impact velocity of 72 m/s and 120 mesh has an impact velocity of 70 m/s.

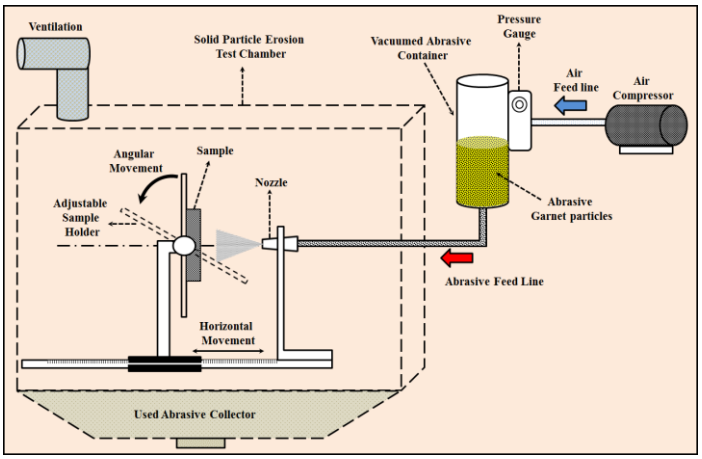


Figure 1. Solid particle erosion test rig

Solid particle erosion test parameters are given in Table 2.

Table 1 : Solid particle erosion test parameters

| **Erodent type** | **Alumina** |
|---|---|
| Erodent size | 60 mesh (212-300 µm)<br>80 mesh (150-212 µm)<br>120 mesh (90-250 µm) |
| Particle impingement angle | 90° |
| Acceleration/blast gun pressure | 3 bar |
| Erodent velocity | 60 mesh (64 m/s)<br>80 mesh (72 m/s)<br>120 mesh (70 m/s) |
| Test temperature | 25 °C ± 2 °C |
| Stand-off Distance | 20 mm |
| Humidity | 50 % |

After solid particle erosion tests, the surfaces of the AA6082-T6 samples were scanned with Nanovea PS50 non-contact 3D profilometer. The erosion crater area of 20 mm × 20 mm scanned with a 10 μm precision. Roughness measurements and related results were obtained from these scans. Roughness parameters such as $R_a$, $R_v$, $R_z$, $S_a$ and erosion crater volume were discussed.

## 3. Discussion on Results

Figure 2 illustrates the erosion rates of AA6082-T6 aluminum alloys tested with 60, 80 and 120 mesh alumina abrasive particles. Abrasive particle grain size has a considerable effect on erosion rate of AA6082-T6 aluminum alloy test coupons. As the grain size of the abrasive particles decrease, the erosion rate increases as seen in Figure2.

Minimum erosion rate observed in tests conducted with 60 mesh alumina abrasive particles whilst the maximum erosion rate occurred in 120 mesh alumina particles. Smaller particles as in 120 mesh enhances material removal from target material due to repeating impacts of abrasive particles. Tests with 60 mesh alumina particles (212-300 μm) resulted with an erosion rate of 19 whilst 120 mesh particles (90-250 μm) resulted with an erosion rate of 90. Hence, decreasing abrasive particle size increases erosion rate approximately 4 times.

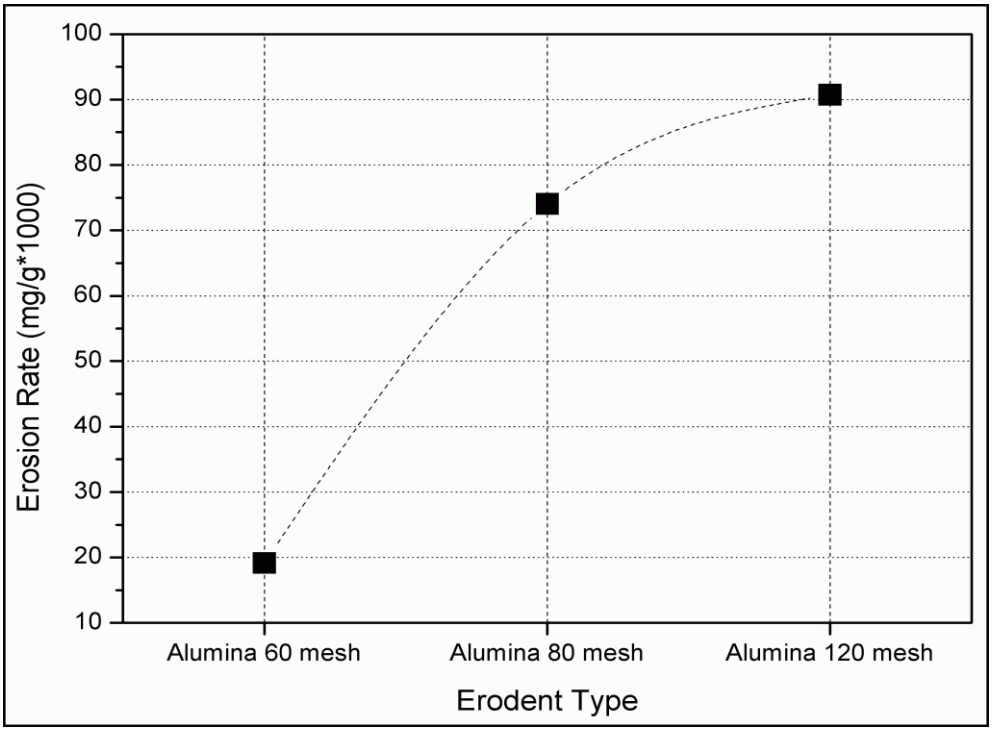


Figure 2. AA6082-T6 aluminum alloy erosion rate versus erodent type

Figure 3 illustrates the 3D surface roughness maps of AA6082-T6 aluminum alloys tested with 60, 80 and 120 mesh alumina abrasive particles. Surface scanning with laser profilometer gives the average roughness of surface named $S_a$. In Figure 3, erosion crater surface region boundaries were clearly be seen with 3D surface maps. Pitting region around the center of erosion crater can also be seen. Maximum $S_a$ was observed in samples tested with 80 mesh particles while minimum $S_a$ observed in 60 mesh abrasive particles. Eroded with 80 and 120 mesh abrasive alumina particles gave similar $S_a$ values. In Figure 3, 120 mesh erosion crater has a deeper damage zone while pitting region around the center has smoother characteristic. Moreover, 60 and 80 mesh abrasive particles resulted with a shallow crater center but a dramatic pitting damage zone around the center damage zone. $S_a$ implies the overall surface roughness, the $S_a$ values were almost similar for all abrasive particles.

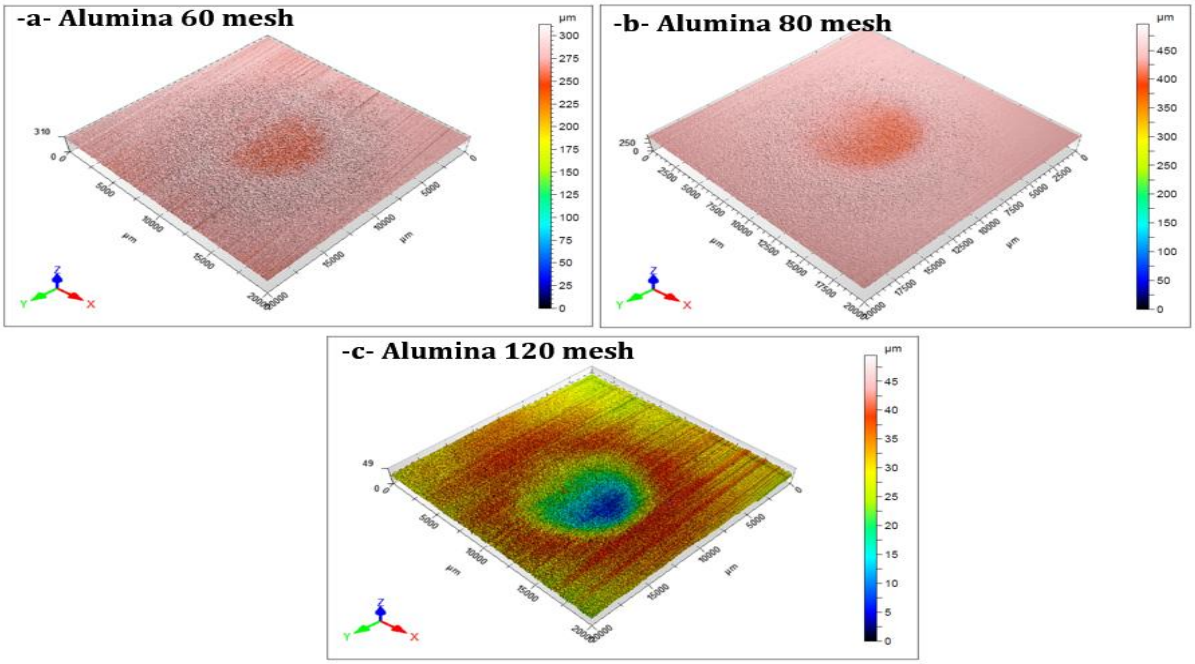


Figure 3. 3D surface roughness maps of AA6082-T6 aluminum alloy after erosion tests

Figure 4 illustrates the line roughness of AA6082-T6 aluminum alloys tested with 60, 80 and 120 mesh alumina abrasive particles taken from the center of the tested samples. On the left, the location of the line illustrated on the surface of the test coupons and on the right side, the roughness profile was shown in thickness axis. As in Figure 4-a, AA6082-T6 test samples eroded with 60 mesh alumina abrasive particles caused a shallow erosion crater center. Big abrasive particles interact with each other during their flight from nozzle exit to sample surface and their kinetic energy decreases because of this interaction. Hence hitting sample surface with a lower kinetic energy resulted with shallow erosion crater center. Moreover, erosion with 80 and 120 mesh abrasive particles enhances erosion crater center depth. Repeated impacts of particles on the center region enhances $R_v$ value. Around the center erosion crater region, a circular region of peaks observed. Peaks around the center region implies the plastic deformation on AA6082-T6 aluminum alloy surface. Peaks are various sized elevations from the reference samples.

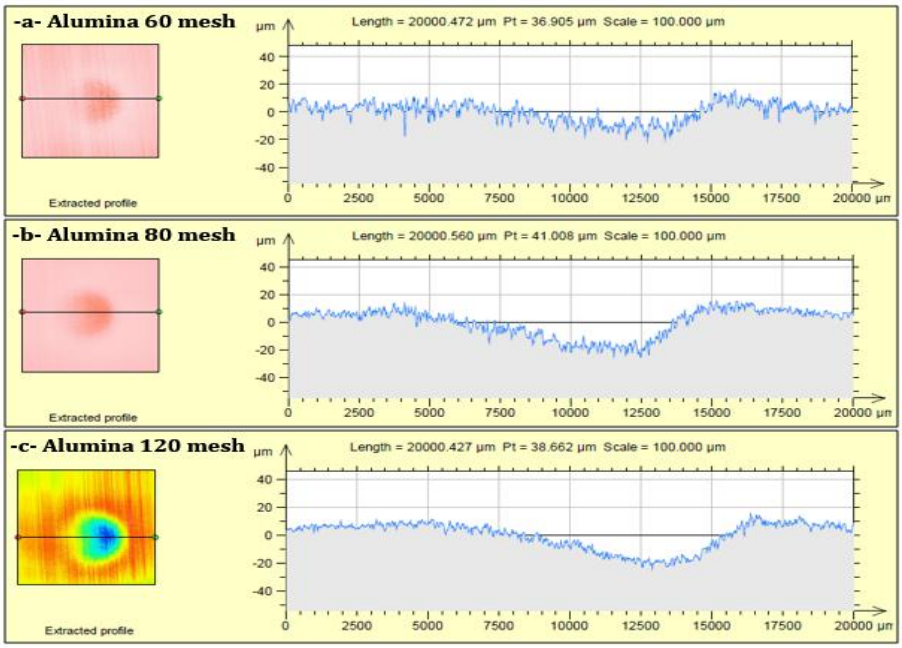


Figure 4. Surface roughness center profiles of AA6082-T6 aluminum alloy after erosion tests

Figure 5 illustrates various roughness parameters such as $R_a$, $R_v$, $R_z$ and $S_a$ of AA6082-T6 aluminum alloys tested with 60, 80 and 120 mesh alumina abrasive particles. As it can be seen in Figure 5, decreasing abrasive particle size from 60 mesh to 120 mesh decreases the $R_a$, $R_v$ and $R_z$ values. $R_a$ value implies the average roughness of tested samples. $R_v$ implies the roughness values in valley occurred in sample surfaces after solid particle erosion tests. $R_z$ implies the average of vertical distance between top of the peaks and bottom of the valleys occurred in sample surfaces after solid particle erosion tests. Unlike $R_a$, $R_v$ and $R_z$ values, $S_a$ value increases with decreasing abrasive particle size. This result can be attributed to meaning of $S_a$ value because it implies average roughness of whole tested sample whilst $R_a$, $R_v$ and $R_z$ values are obtained from linear roughness profile. Moreover, variation in $S_a$ value was slight. So, abrasive particle size has a little effect on $S_a$ value.

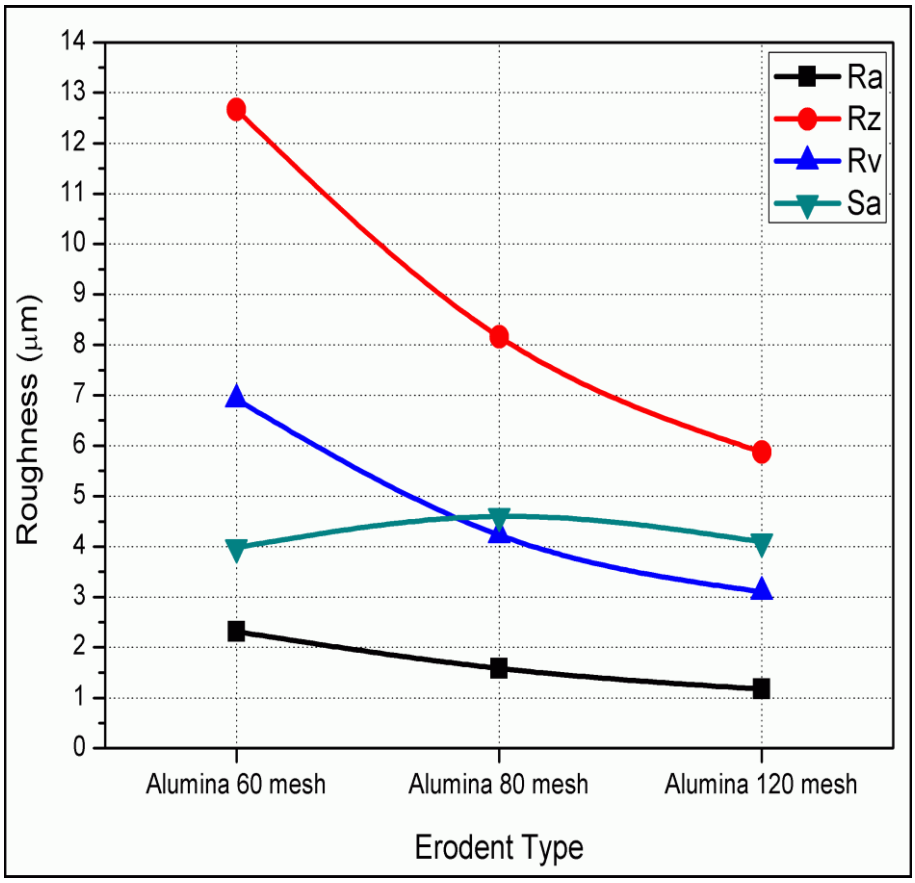


Figure 5. Roughness values of AA6082-T6 aluminum alloy after erosion tests

Figure 6 illustrates erosion crater volumes of AA6082-T6 aluminum alloys tested with 60, 80 and 120 mesh alumina abrasive particles. As seen in Figure 6, biggest erosion crater volume occurred after erosion tests conducted with 60 mesh alumina particles. On the other hand, minimum erosion rate observed in 60 mesh abrasive particles. Hence, although minimum erosion rate observed with 60 mesh; maximum erosion crater volume observed also with 60 mesh. This conclusion can be attributed to plastic deformation. Big sized abrasive particles caused severe erosion crater volume. Reversely, minimum erosion crater volume observed in samples eroded with 120 mesh alumina abrasive particles which have the maximum erosion rate. Small abrasive particles caused a smaller erosion crater volume. As a result, abrasive particles with a bigger size caused a significant erosion crater volume whilst smaller abrasive particles resulted with a smaller erosion crater volume.

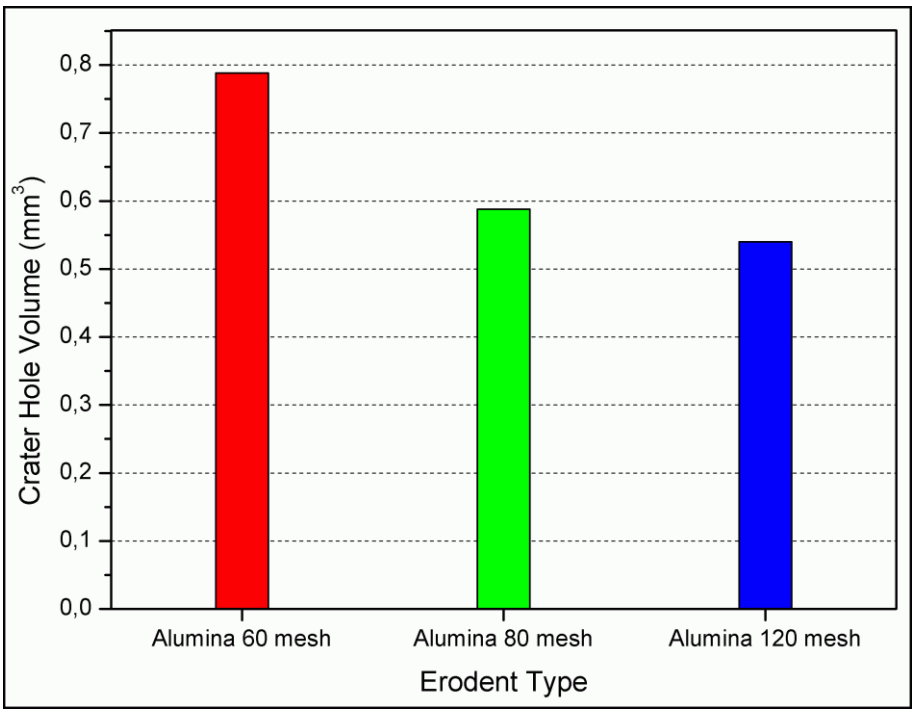


Figure 6. Erosion crater volume of AA6082-T6 aluminum alloy after erosion tests

## 4. Conclusions

The main conclusions drawn from the present work can be summarized as follows:

- AA6082-T6 aluminum alloy samples eroded with 60 mesh alumina abrasive particles have minimum erosion rate whilst samples eroded with 120 mesh alumina particles have the maximum erosion rate after solid particle erosion tests. Hence, decreasing abrasive particle size increases erosion rate for AA6082-T6 aluminum alloy.
- After erosion tests of AA6082-T6 aluminum alloy samples, roughness comparison was accomplished. Decreasing abrasive particle size from 60 mesh to 120 mesh decreases the $R_a$, $R_v$ and $R_z$ values. Unlike $R_a$, $R_v$ and $R_z$ values, $S_a$ value increases with decreasing abrasive particle size. Moreover, variation in $S_a$ value was slight. So, abrasive particle size has a little effect on $S_a$ value.
- Biggest erosion crater volume occurred after erosion tests conducted with 60 mesh alumina particles. On the other hand, minimum erosion rate observed in 60 mesh abrasive particles. Big sized abrasive particles caused severe erosion crater volume. Reversely, minimum erosion crater volume observed in samples eroded with 120 mesh alumina abrasive particles which have the maximum erosion rate. Small abrasive particles caused a smaller erosion crater volume.

## Acknowledgment

Extruded AA6082-T6 aluminum sheets are kindly supplied from ASAŞ Aluminum A.Ş. TURKEY. Authors are very thankful for the materials and collaboration of R&D Center of ASAŞ Aluminum. Solid particle erosion tests and profilometer scans were accomplished in Wear Laboratory of Kocaeli University, Faculty of Aeronautics and Astronautics.

## References

[1] H. Arabnejad, A. Mansouri, S. Shirazi, and B. McLaury, "Development of mechanistic erosion equation for solid particles," *Wear*, vol. 332-333,pp. 1044-1050, 2016.

[2] M. Takaffoli and M. Papini, "Numerical simulation of solid particle impacts on Al6061-T6 part II: Materials removal mechanisms for impact of multiple angular particles," *Wear*, vol. 296, no. 1-2, pp. 648-655, 2012.

[3] A. Algahtani, A. Neville, S. Shrestha, and T. Liskiewicz, "erosion resistance of surface engineered 6000 series aluminium alloy," *Proc. Inst. Mech*. Eng. Part J J. Eng. Tribol. , vol. 227, no. 11, pp. 1204-1214, 2013.

[4] M. Trevino, R. D. Mercado-Solis, R. Colas, A. Perez, J. Talamantes, and A. Velasco, "Erosive wear of plasma electrolytic oxidation layers on aluminium alloy 6061, " *Wear*, vol. 301, no. 1-2, pp. 434-441, 2013.